

### **Optical Characteristics of Amorphous Tin Nitride Thin Films Prepared by Ion Beam Assisted DC Magnetron Reactive Sputtering**

**I. M. Odeh**

*Physics Department, Yarmouk University, Irbid 21163, Jordan.*

---

*Received on: 7/12/2007; Accepted on: 5/6/2008*

---

**Abstract:** This work reports the preparation of thin films of amorphous tin nitride (a-Sn:N) by a novel implementation of simultaneous ion beam assisted deposition (IBAD) and reactive DC magnetron sputtering of a metal tin target in pure nitrogen plasma. The work also reports the optical characterization and determination of the optical constants of a-Sn: N thin film material. The refractive index  $n$  varies only slightly over the spectral range of 400-900 nm while the extinction coefficient  $k$  displays a gradual but significant increase starting at  $\sim 470$ nm. We have estimated the optical energy gap,  $E_{opt}$ , to be  $2.32 \pm 0.047$ eV deduced from the transmittance measurements. Other important optical characteristics, such as the high frequency dielectric constant  $\epsilon_{\infty}$ , the average oscillator's wavelength  $\lambda_o$ , the average oscillator strength  $S_o$ , tangent loss ( $\tan \delta$ ) and the optical conductivity  $\sigma$ , are also determined. Determination and interpretation of some of the optical properties are based on the single oscillator model proposed by Wemple and DiDomenico.

**Key Words:** Amorphous Materials, Reactive Sputtering, Ion Beam Assisted Deposition (IBAD), Thin Films, Optical Properties.

#### **Introduction**

Crystalline Tin (IV) Nitride of the form  $\text{Sn}_3\text{N}_4$ , non-stoichiometric  $\text{SnN}_x$  and  $\text{Sn}_x\text{N}_y$  in thin film forms have attracted the attention of a considerable number of researchers because of the potential applications of this material and their semi-conducting electrochromic properties. These include optical storage devices, write-once optical recording media, applications in microelectronic devices, as materials for optical switching devices for solar energy purposes, and optical recording media.  $\text{Sn}_3\text{N}_4$  is also one of the Nitrides of the fourth group of the periodic table, which received much interest after the findings of the significant physical characteristics and the chemical properties [1-6].

Preparation methods of the various forms, powder and thin films, of tin nitrides varied from chemical procedures [7-9] to physical methods including reactive sputtering [2, 3, 10-14], reactive ion plating

[15], chemical vapor deposition [16] and plasma enhanced CVD [17].

Structural, optical, and electronic properties of almost any material, particularly thin films, depend essentially on the preparation technique. This is also true for the various forms of tin nitrides.

Most of the research works in the published literature have concentrated mainly on the crystalline forms of tin nitride produced by different methods [1-17].

In a review of the group (IV) nitrides, Kroke and Schwarz [18] mentioned that very few reports on tin nitride phases appeared in the literature. The electrical and optical characteristics of non-stoichiometric ( $\text{SnN}_x$ ) crystalline tin nitride films have been examined for solar energy purposes [5, 19]. Maruyama and Morishita [12] reported a band gap of 1.5 eV for the crystalline  $\text{SnN}_x$ . Recent theoretical calculations [20] predict that  $\gamma$ - $\text{Sn}_3\text{N}_4$ , in the spinel structure, is a semiconductor with a direct band gap of

1.40 eV and an attractive small electron effective mass of  $0.17 m_0$ .

Only a very limited number of research papers reported specifically on the amorphous tin nitride [21-23]. However, a thorough investigation of the optical characteristics, namely the refractive index, the absorption coefficient, dielectric constant and the optical energy gap of this interesting material in particular is not available.

We have prepared and studied the optical properties of amorphous tin nitride as a part of an ongoing research in the area of amorphous metal nitrides [24], and because of the need to explore the properties of alternative optical materials with potential applications. Our contribution to studying this type of film material takes a different approach in the deposition method, the structure form, and the method of determining the optical characteristics. Here we combine the ion beam assisted deposition (IBAD) and reactive DC magnetron sputtering for the deposition of the films. This novel approach [24] to preparation of thin films has produced amorphous tin nitride films that are compatible with the crystalline tin nitride films in some aspects of the optical characteristics and stability at room temperature conditions.

The optical constants,  $n$ , and  $k$ , of thin films are fundamental parameters both from theoretical and practical points of view. These provide essential information on the optical energy gap for semiconductors and insulators. Furthermore, the refractive index is necessary for the design and modeling of optical components and optical coatings [25].

In this work, we place a particular emphasis on the optical properties of the amorphous a-Sn: N films in comparison with the crystalline  $\text{Sn}_3\text{N}_4$ . For calculating the optical constants and thicknesses of a-Sn:N thin films from transmittance measurements, we have applied the PUMA method and software [26], which has proved suitable for the purpose of retrieving the optical constants from transmittance measurements only [25].

### Experimental Details and Preparation Conditions

The tin nitride films were deposited onto glass and silicon substrates in an Edwards E306 coating system fitted with an Edwards sputtering accessory (75 mm Magnetron

Cathode E093-01-000). An End-Hall ion beam source [27] was specifically designed, built, and retrofitted to the vacuum chamber (in house) in such a way that the ions produced would impinge onto the films during deposition process. A novel substrate holder (Hexa-holder) capable of loading six substrates simultaneously was also designed and constructed (in house) specifically for this work. The holder rotates at controlled speeds in a fashion such that the substrates always face the sputtering target one at a time during deposition. Ions from the ion beam source bombarded the substrate during deposition. In this way low energy ions ( $<100\text{eV}$ ) would impart enough energy during the film deposition which would enhance the quality of the deposited films. This also improved the adhesion of the film to the substrate.

The substrates were thoroughly cleaned by first washing in a detergent (Decon5) and de-ionized water followed by rinsing in alcohol. All cleaning steps were carried out in an ultrasonic bath. To insure maximum cleaning and to remove oxides and contamination, both substrates and sputtering target were further bombarded with argon ions from the ion beam source for several minutes prior to deposition.

A 1kW DC power supply (MDX 1K Magnetron Drive from Advanced Energy, USA) delivered the DC power to the water-cooled tin target. An independent power supply (HP 6521A) and a low-tension transformer provided the necessary power to the ion source during deposition.

The spacing between the target and substrate was always maintained at 5cm. Reactive sputtering was carried out at room temperature in a glass bell jar vacuum chamber. The chamber was backfilled with pure nitrogen and maintained at a pressure of  $\sim 100$  mbar during deposition. The power applied to the tin target was 100W dc. The vacuum chamber was always pumped down to better than  $10^{-5}$  mbar and flushed with nitrogen to remove any residual oxygen prior to deposition.

As a routine procedure, we have performed the following characterization experiments on the as-deposited films.

### X-ray Diffraction (XRD)

To establish the structure of the films whether crystalline or amorphous; X-ray diffraction (XRD) measurements were carried out using a computer controlled

Phillips PW1710 Diffractometer equipped with copper tube, for CuK $\alpha$  radiation, and a theta compensatory slit assembly. The diffractometer was operated under the following experimental conditions: a voltage of 35 kV, beam current of 40mA, step size of 0.02 2 $\theta$ , counting time of 0.01sec/step, 1mm receiving slit and a scanning range of 5-100 $^{\circ}$  2 $\theta$ .

### Transmittance Measurements

Transmittance (%T) of the as deposited tin nitride films was measured in a UV-Visible double-beam spectrophotometer over a spectral range of 400-900nm. The transmittances of the films were recorded with a blank substrate placed in the reference beam path.

### Experimental Results and Discussion

Fig.1 shows a representative X-ray diffraction spectrum of the Tin Nitride (SnNx) films on glass substrates. The Tin Nitride films prepared here clearly do not display

any well-defined peaks, which are typical of crystalline structures. It is clear from the figure that the ion beam assisted DC magnetron reactive sputtering has produced amorphous films. Quantitative estimate of the composition from the data is not a straightforward conclusion. Therefore, the exact atomic ratio of the sputtered SnNx is unknown. However, since the films were prepared by sputtering from a pure tin target in pure nitrogen plasma, and all samples were non-metallic, as was deduced from the optical transmittance, it was clear that a reaction occurred and some sort of SnNx was present in the films. Nevertheless, Energy Dispersive X-ray analysis (EDX), a well known technique used for identifying the elemental composition of an area of the film and an integrated feature of the scanning electron microscope (SEM), revealed that x~3 in some of the films. Maruymama et al. [12] produced amorphous SnNx films at comparable conditions, except for the use of IBAD.

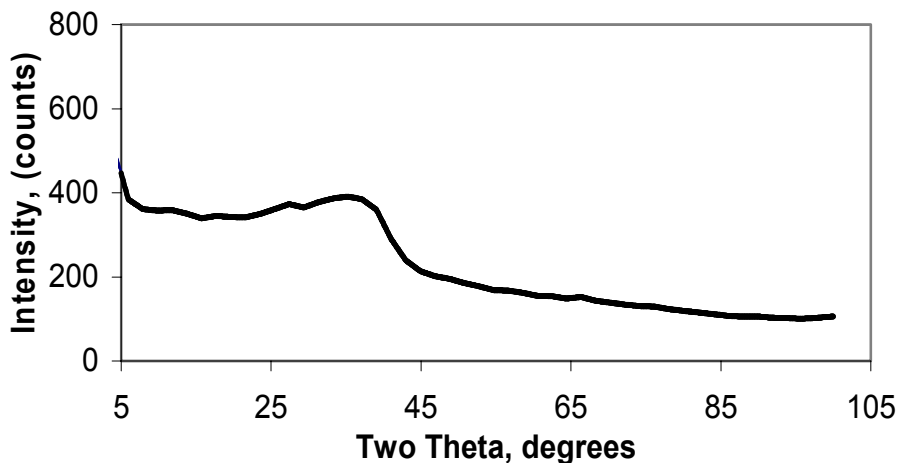
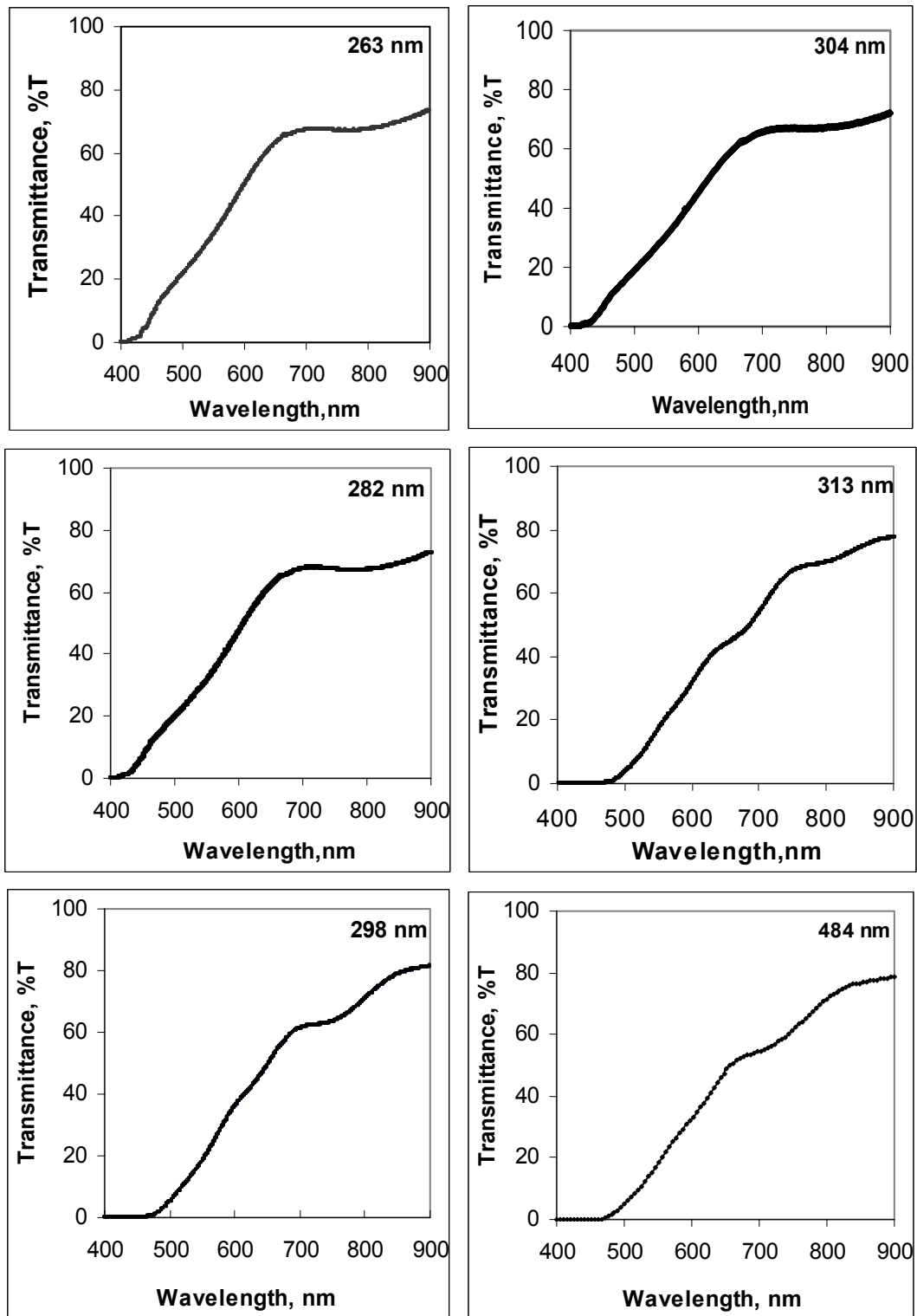


Fig. 1: A typical XRD pattern (Smoothed) of the a-Sn: N thin films on a glass substrate. The broad peak is due to the glass substrate.

Fig.2 shows transmittance spectra over a wavelength range of 400-900 nm for a representative set of films deposited at similar preparation conditions of nitrogen pressure (~100mbar) and dc power (~100W) over various time durations. The tin nitride films show almost invariably low optical transmittance over the visible range but

higher transmittance over the near infrared range. The spectra exhibit a behavior typical of the amorphous thin films where a broad absorption is evident compared to sharp absorption that usually characterizes crystalline materials. The films have a clear yellow to brown coloring depending on the thickness of films.



**Fig. 2:** Transmittances (%T) of a number of a-Sn: N thin films of different thicknesses (263- 484 nm) over the spectral range of interest (400-900 nm).

### The Optical Constants: the Refractive Index $n$ and Extinction Coefficient $k$

Determination of the real part,  $n$ , and the imaginary part,  $k$  of the complex refractive index is a challenging task when it comes to studying the optical properties of materials. The procedure involves complex equations

and extensive computing. A number of approaches and different methods exist for determining the optical constants [28-36].

The easiest are those, which depend on single transmittance measurement [25]. The refractive index  $n$  and the extinction coefficient  $k$  as well as the thickness  $d$  of the

amorphous tin nitride films studied here were determined from the transmittance data only using Point-wise Unconstrained Minimization Approach for the estimation of the thickness  $d$  and optical constants  $n$  and  $k$  of thin films (PUMA) approach and software [26]. It is a procedure and software

described by Birgin et al [26]. This method implements the complex optical equations derived and formulated by Heavens [29] and Swanepool [31, 32]. The transmission  $T$  of a thin absorbing film deposited on a thick transparent substrate is given by:

$$T = [Ax / (B - Cx + Dx^2)] \quad (1)$$

where:

$$A = 16n_s (n^2 + k^2)$$

$$B = [(n+1)^2 + k^2][(n+1)(n+n_s^2) + k^2]$$

$$C = [(n^2 - 1 + k^2)(n^2 - n_s^2 + k^2) - 2k^2(n_s^2 + 1)]2 \cos \theta \\ - k[2(n^2 - n_s^2 + k^2) + (n_s^2 + 1)(n^2 - 1 + k^2)]2 \sin \theta$$

$$D = [(n-1)^2 + k^2][(n-1)(n-n_s^2) + k^2]$$

$$\beta = 4\pi nd / \lambda$$

$$x = \exp(-\alpha d)$$

$$\text{And } \alpha = 4\pi k / \lambda$$

Where  $n_s$  is the refractive index of the substrate,  $n$  and  $k$  are the real and imaginary parts of the refractive index of the film respectively,  $d$  is the film thickness,  $\lambda$  is the wavelength of the incident light and  $\alpha$  is the absorption coefficient of the film.

The substrate is sufficiently thick such that the additional interference effects resulting from the multiple reflections in the substrate are eliminated because they are incoherent.

In PUMA, the experimental transmittance obtained for the film is compared with a theoretical value. The difference between the two values is minimized until a best solution is reached for the refractive index  $n$ , the extinction coefficient  $k$  and the film thickness  $d$ . Thicknesses of the films

determined from PUMA calculations and based on the transmittances of the films ranged from 263 to 484 nm. Poelman et al [25] have reviewed and tested his method independently and shown it to produce excellent estimates of optical parameters of thin films.

Fig.3 shows average values of the refractive index  $n$  and the extinction coefficient  $k$  as a function of photon energy over the spectral range 400-900nm. The figure clearly shows that the refractive index exhibits only very slight increase over the spectral range. The extinction coefficient  $k$  displays a knee above 2.3eV (below 540nm). We attribute this change to higher dispersion and strong absorption of the tin nitride films at that wavelength.

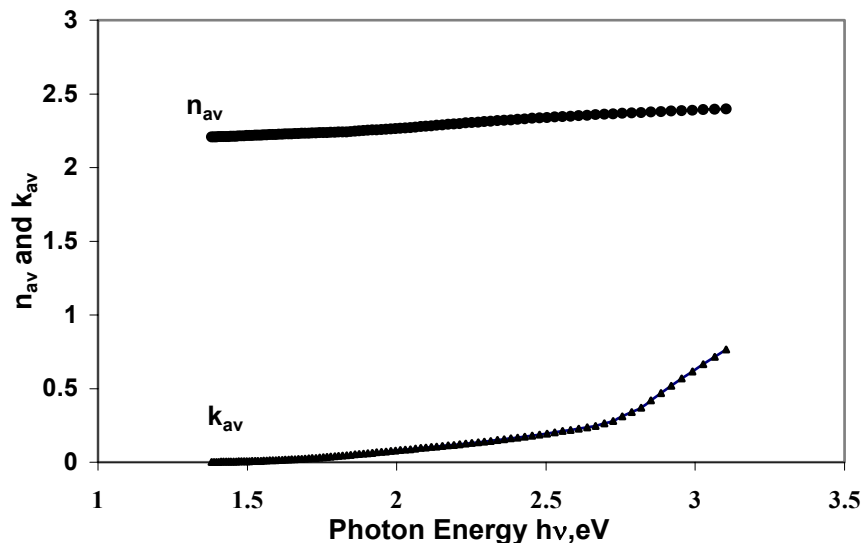


**Fig. 3:** Plots of  $n$  and  $k$ , the real refractive index and the extinction coefficient respectively, versus photon energy of the spectral range of interest (400-900 nm) for the a-Sn: N thin films.

A plot, Fig.4, of a typical absorption coefficient  $\alpha$  of the tin nitride over the same spectral range clearly shows this inflection in the absorption. Nevertheless, it is not sharp

enough to resemble the sharp absorption of a crystalline material but consistent with amorphous thin film materials.

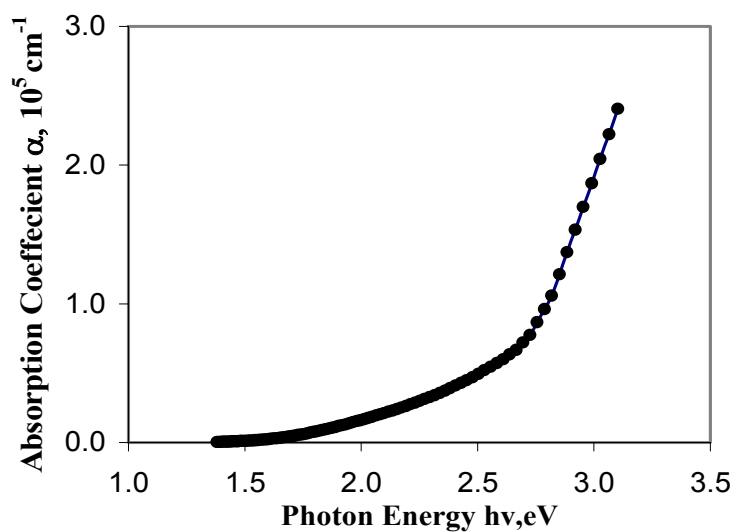


**Fig. 4:** A typical plot of the absorption coefficient,  $\alpha$ , as a function of the photon energy of the spectral range of interest (400-900 nm).

In order to establish the optical transitions involved in the films, a plot of  $\log(\alpha h\nu)$  against  $\log(1/\lambda)$  should yield one straight line for a single optical transition. However if the plot should produce more

than one line then this would indicate multiple transitions [37].

Fig.5 shows such a plot, where it produced a single line, clearly indicating a single optical transition. We will show below that this is consistent with indirect transition.

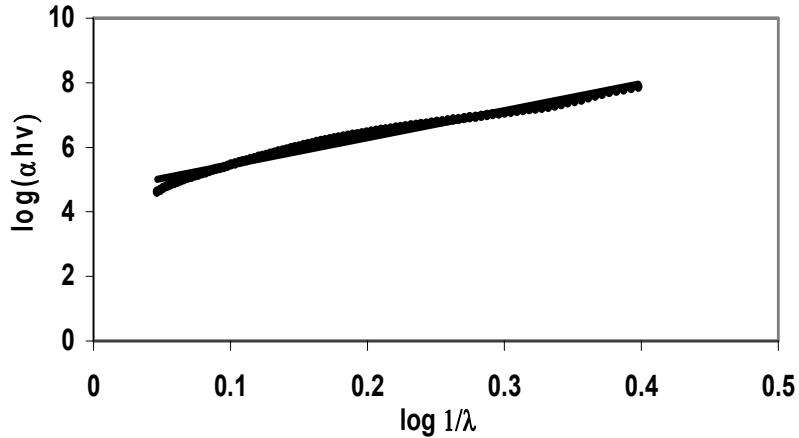


Fig. 5: A plot of  $\log(\alpha h\nu)$  versus  $\log(1/\lambda)$  shows a single line indicating a single optical transition.

### The Optical Energy Gap $E_{opt}$

The optical energy gap  $E_{opt}$  is another important quantity that characterizes semiconductors and dielectric materials since it has a paramount importance in the design and modeling of such materials [25]. For the amorphous tin nitride films studied here, the optical energy gap was deduced from the intercept of the extrapolated linear part of the plot of  $(\alpha h\nu)^{1/2}$  versus the photon energy  $h\nu$  as abscissa. This followed from the method of Tauc et al [38] where

$$(\alpha h\nu)^{1/2} = \text{constant}(h\nu - E_{opt}) \quad (2)$$

Fig.6 displays plots of  $(\alpha h\nu)^{1/2}$  versus photon energy  $h\nu$  for a number of representative a-Sn: N films. The plot is a straight line as a best fit of the Tauc's relation above which suggests an indirect optical transition. An average value of optical energy gap  $E_{opt}$  of  $2.320 \pm 0.047\text{eV}$  is calculated from the intercepts of the extrapolated lines with photon energy axis for the amorphous tin nitride films. The results of Fig.5 support a single optical

indirect transition. The value of the optical energy gap for the amorphous films is greater than the optical energy gap of 1.5 eV reported for the crystalline tin nitride  $\text{Sn}_3\text{N}_4$  thin films prepared by radio frequency reactive sputtering [2, 3]. A recent ab initio calculation of the electronic structure and spectroscopic properties of spinel  $\gamma$ - $\text{Sn}_3\text{N}_4$  report that this is a semiconductor with a direct band gap of 1.40 eV [20].

The higher optical energy gap estimated in this work for a-Sn: N is consistent with the nature of the amorphous materials characterized by the absence of long-range order, high resistivity, and presence of defects. We believe that the bombardment of the films with low energy nitrogen ions from the ion source during deposition has contributed to the formation of the amorphous structure in addition to improving the quality, stability at laboratory conditions, and homogeneity of the amorphous films. Zeng et al [39] reported ion beam induced growth of amorphous alloy films of Co-Nb system by ion beam assisted deposition.

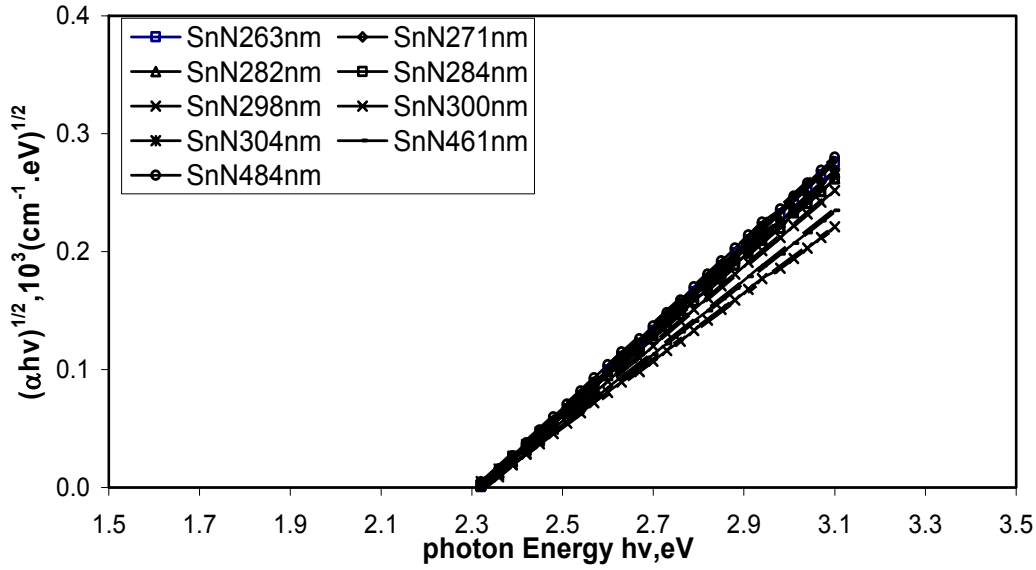


**Fig. 6:** Plots of  $(\alpha hv)^{1/2}$  versus photon energy,  $hv$ , for a-Si:N illustrating the intercepts of the extrapolated linear part with the photon energy axis. An average estimate for the optical gap is  $E_{opt} = 2.320 \pm 0.047\text{eV}$  for a number of films.

The above result of the optical energy gap may be further confirmed based on the following relation [40-43].

$$h^2 \nu^2 \epsilon_2 \sim (h\nu - E_{opt})^2 \quad (3)$$

where  $\epsilon_2 (= 2nk)$  is the imaginary part of the dielectric constant.

A plot of  $h\nu(\epsilon_2)^{1/2}$  versus photon energy exhibits a linear relation. This gives the optical gap when extrapolated to the energy axis. Fig.7 shows such a plot where the extrapolated linear part yields an optical energy gap of 2.28 eV in excellent agreement with the value  $2.320 \pm 0.047\text{eV}$  obtained from the plot in Fig.6.

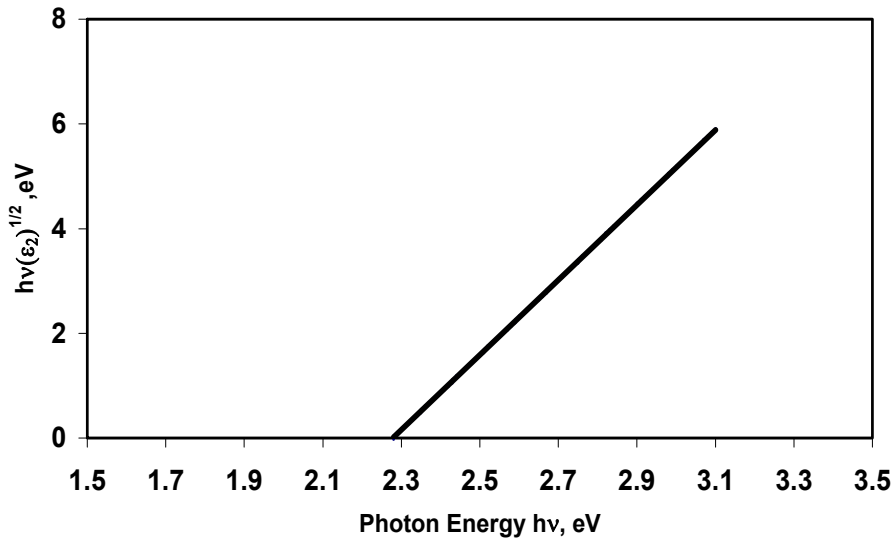


**Fig. 7:** A plot of  $h\nu(\epsilon_2)^{1/2}$  versus photon energy,  $hv$ , for a-Sn: N illustrates the intercepts of the extrapolated linear part with the photon energy axis. An estimate of optical gap is  $E_{opt} = 2.28\text{ eV}$ .

### Analysis of Dispersion of Films

Dispersion, the frequency dependence or energy dependence of the refractive index, can be analyzed based on the concept of a single oscillator model proposed by Wemple

and DiDominico [41, 42]. In this model, the following relation expresses the energy dependence of the refractive index,  $n$  as:

$$n^2 = 1 + E_d E_o / (E_o^2 - E^2) \quad (4)$$



where  $E (=hv)$ ,  $E_o$  and  $E_d$  are the photon energy, the oscillator energy and the dispersion energy respectively. The parameter  $E_d$  is a measure of the intensity of the interband optical transition. It is independent of the optical band gap [44]. Fig.8 illustrates a plot of the dispersion relation (4) where  $(n^2-1)^{-1}$  is plotted versus  $E^2$  for the a-Sn: N films. Extrapolation of the lower energy part of the spectral range

where the films are more transparent displays a linear trend as shown in Fig.8. Dispersion energy  $E_d$  and oscillator energy  $E_o$  are estimated from the slope of -0.0077 and the intercept of 0.273 of the extrapolated linear part. We find these estimates from the equation of the best linear fit to be  $E_d = 21.81\text{eV}$  and  $E_o = 5.95\text{ eV}$ . In addition, we find an estimate for the optical dielectric constant  $\epsilon_\infty = n_\infty^2 = 4.664$ .

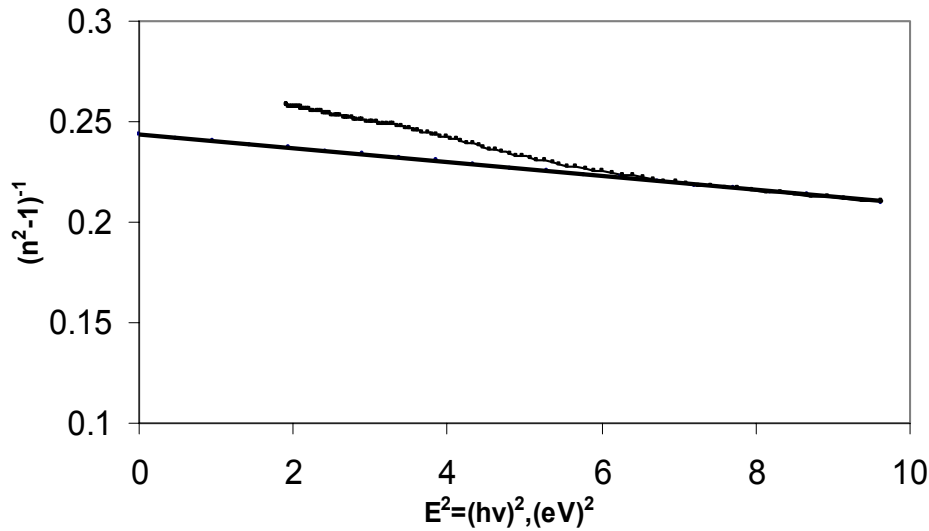


**Fig. 8:** A plot of the dispersion relation (4) where  $(n^2-1)^{-1}$  is plotted versus  $E^2 = (hv)^2$  for the a-Sn: N films.

The refractive index  $n$ , the wavelength  $\lambda$  and the lattice dielectric constant  $\epsilon_L$  are related through the relation (5), which takes into consideration the contribution of the free carriers and the lattice vibration modes [44, 45]:

$$n^2 = \epsilon_L - C\lambda^2 \quad (5)$$

where  $C = (e^2 N / 4\pi^2 c^2 \epsilon_o m^*)$ ,  $\epsilon_L$  is the lattice dielectric constant,  $e$  is the electronic charge,  $N$  is the concentration of the free charge carriers,  $\epsilon_o$  is the vacuum permittivity,  $m^*$  is the effective mass of the charge carrier,  $c$  is the speed of light and  $\lambda$  is the photon wavelength.

### Conclusions

We have prepared thin films of amorphous tin nitride by a novel implementation of reactive DC magnetron sputtering and ion beam assisted deposition simultaneously. This technique has produced high quality, stable and uniform amorphous films. The bombardment of the film during deposition with low energy ions played a major role in producing the amorphous structure through imparting energies to the accumulating atoms. The

XRD patterns of films, Fig.1, clearly support this conclusion where the typical sharp peaks of crystalline structures are absent. Amorphous and crystalline tin nitrides both have similar yellow coloring for thinner films and dark brown for thicker films. The refractive index varied only slightly over the wavelength range of interest, 400-900 nm. The films are not highly absorptive over the visible part of the same spectral range.

A distinct difference between the amorphous and the crystalline tin nitrides is the invariably higher optical energy gap determined for the amorphous films of  $2.320 \pm 0.047\text{eV}$  compared with the inconsistent values, 1.4-1.5 eV, for the crystalline films. The amorphous films have shown stability and have sustained normal lab and room temperature conditions for very long periods. Based on the optical properties presented in this work we believe that amorphous tin nitride may have potential applications as a decorative material, UV absorber and to a lesser extent as a hard coating.

## Acknowledgements

We would like to thank the Deanship of Scientific Research and Higher Studies at Yarmouk University for the financial support. We would also like to thank Mosa Al-Jabali and A. Shehadeh from the Workshop at the physics Department, Yarmouk University.

## References

- [1] T. Maruyama and Y. Osaki. (1996). *J. Electrochem. Soc.* 143, 326.
- [2] T. Maruyama and T. Morishita. (1996). *Appl. Phys. Lett.* 69, 890.
- [3] Y. Inoue, M. Nomiya and O. Takai. (1998). *Vacuum*, 51, 673.
- [4] Naoyuki Takahashi, Masahisa Takekawa, Tadashi Takahashi, Takato Nakamura, Masayuki Yoshioka, Wataru Inami and Yoshimasa Kawata. (2003). *Solid State Sciences*, 5, 587–589
- [5] N. Takahashi, K. Terada, T. Takahashi, T. Nakamura, W. Inami and Y. Kawata. (2003). *J. Electron. Mater.* 32, 268.
- [6] H. Lange, G. Wötting and G. Winter. (1991). *Angew. Chem.* 103, 1606.
- [7] L. Maya. (1992). *Inorg. Chem.* 31, 1958.
- [8] N. Scotti, H. Jacobs, W. Kockelmann and Z. Anorg. (1999). *Allg. Chem.* 625, 1435-1439.
- [9] M. P. Shemkunus, G. H. Wolf, K. Leinenweber and W. T. Petuskey. (2002). *J. Am. Ceram. Soc.* 85, 101.
- [10] J. C. Remy and J. J. Hantzpergue. (1975). *Thin Solid Films* 30, 197.
- [11] R. S. Lima, P. H. Dionisio, W. H. Schreiner and C. Achete. (1991). *Solid State Commun.* 79, 395.
- [12] T. Maruyama and T. Morishita. (1995). *J. Appl. Phys.* 77, 6641.
- [13] R. Kamei, T. Migita, T. Tanaka and K. Kawabata. (2000). *Vacuum*, 59, 764.
- [14] H. M. Al-Mosawi. (1999). MSc thesis, Yarmouk University,
- [15] Y. Inoue, Y. Fukui and O. Takai. (1994). *Proc. Symp. Plasma Sci. Mater.* 7, 147.
- [16] R. G. Gordon, D. M. Hoffman and U. Riaz. (1992). *Chem. Mater.* 4, 68.
- [17] D. M. Hoffman, S. P. Rangarajan, S. D. Athavale, D. J. Economou, J. R. Liu, Z. Zheng and W. K. Chu. (1995). *J. Vac. Sci. Technol.*, A 13, 820.
- [18] E. Kroke and M. Schwarz. (2004). *Coordination Chemistry Reviews*, 248, 493–532.
- [19] T. Lindgren, M. Larsson and S. E. Lindquist. (2002). *Solar Energy Mater. Solar Cells* 73, 377.
- [20] W. Y. Ching and P. Rulis. (2006). *Physical Review B* 73, 045202-1-9.
- [21] Y. Inoue, Y. Fukui and O. Takai. (1994). *Proc. Symp. Plasma Sci. for Materials*, 7, 147.
- [22] Y. Inoue and O. Takai. (1996). *Proc. Symp. Plasma Sci. for Materials*, 9, 39.
- [23] Dirk Lu'tzenkirchen-Hecht\* and Ronald Frahm. (2005). *Thin Solid Films*, 493, 67 – 76.
- [24] I. M. Odeh. (2007). Fabrication and optical constants of amorphous copper nitride thin films prepared by ion beam assisted dc magnetron reactive sputtering. In press. *Journal of Alloys and Compounds*, doi:10.1016/j.jallcom.2006.12.020.
- [25] D. Poelman and P. F. Smet. (2003). *J. Phys. D: Appl. Phys.* 36, 1850–1857.
- [26] E. G. Birgin, I. Chambouleyron, and J. M. Martínez. (1999). *Journal of Computational Physics*, 151, 862-880.
- [27] H. R. Kaufman and R. S. Robinson. (1987). *Operation of Broad-Beam Sources*, Commonwealth Scientific corporation.
- [28] M. Born and E. Wolf. (1980). *Principles of Optics*, Pergamon, London.
- [29] O. S. Heavens. (1991). *Optical Properties of Thin Films*, Dover, New York.
- [30] J. C. Manifacier, J. Gasiot, and J. P. Fillard. (1976). *J. Phys. E: Sci. Instrum.* 9, 1002.
- [31] R. Swanepoel. (1983). *J. Phys. E: Sci. Instrum.* 16, 1214–1222.
- [32] R. Swanepoel. (1984). *J. Phys. E: Sci. Instrum.* 17, 896–903.

- [33] A. R. Forouhi and I. Bloomer. (1986). Phys. Rev. B 34, 7018–26.
- [34] A. R. Forouhi and I. Bloomer. (1988). Phys. Rev. B 38, 1865–74.
- [35] I. Bloomer and R. Mirsky. (2002). Photonics Spectra, 86–92.
- [36] A. R. Forouhi and I. Bloomer. (1991). Handbook of Optical Constants of Solids II, Ed E. D. Palik Boston: Academic, 151–75.
- [37] H. S. Soliman, B. A. Khalifa, M. M. El-Nahass and E. M. Ibrahim. (2004). Physica B 351, 11–18.
- [38] J. Tauc, R. Grigorovici and A. Vanacu. (1966). Phys. Status Solidi 15 627.
- [39] F. Zeng, F. Pan. (2002). Journal of Alloys and Compounds, 335, 181–187.
- [40] M. M. Abdel-Aziz, I. S. Yahia, L. A. Wahab, M. Fadel and M. A. Affi. (2006). Applied Surface Science, 252, 8163–8170.
- [41] M. DiDomenico and S. H. Wemple. (1969). J. Appl. Phys. 40, 720.
- [42] S. H. Wemple and M. DiDomenico. (1971). Phys. Rev. B3, 1338.
- [43] M. G. Hutchins, O. Abu-Alkhair, M. M. El-Nahass and K. Abd El-Hady. (2006). Materials Chemistry and Physics, 98, 401–405
- [44] J. Roberts, A. Marks and W. Alexander. (1985). J. Appl. Optics, 24, 3680 .
- [45] J. N. Zemel, J. D. Jensen and R. B. Schoular. (1965). Phys. Rev. A.140, 330.